



Original Research Paper

Kinetic studies on the synthesis of fuel additives from glycerol using CeO₂-ZrO₂ metal oxide catalyst

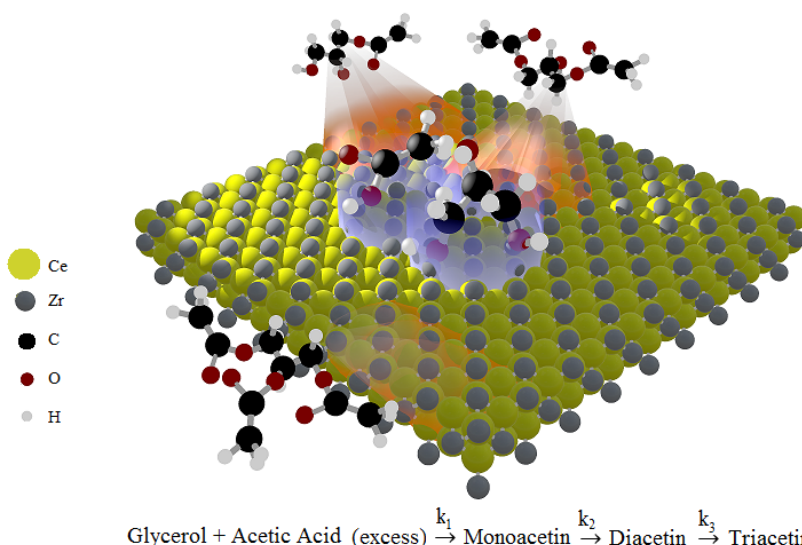
Rajeswari M. Kulkarni*, Pradima J. Britto, Archana Narula, Syed Saqline, Deeksha Anand, C. Bhagyarajlakshmi, R. Nidhi Herle

Department of Chemical Engineering, M. S. Ramaiah Institute of Technology, MSR Nagar, MSRIT Post, Bangalore-560054, Karnataka, India.

HIGHLIGHTS

- Mixed oxide CeO₂-ZrO₂ catalyst in unsulphated and sulphated forms was used for glycerol acetylation to produce acetins (fuel additives).
- Both unsulphated and sulphated mixed oxide catalysts were fully characterized.
- SO₄²⁻/CeO₂-ZrO₂ led to glycerol conversion of 99.12% with selectivity of 57.28% and 21.26% towards di and triacetins, respectively.
- The activation energy for monoacetin, diacetin, and triacetin formation were 5.34, 16.40, and 43.57 kJ.mol⁻¹, respectively.
- Regeneration studies indicated the reusability of the catalyst up to three consecutive cycles.

GRAPHICAL ABSTRACT



ARTICLE INFO

Article history:

Received 21 October 2019
 Received in revised form 11 December 2019
 Accepted 11 December 2019
 Available online 1 March 2020

Keywords:

Biodiesel
 Glycerol
 Fuel additive
 Acetins
 Mixed oxide catalyst
 Kinetic model

ABSTRACT

Highly stable and active CeO₂-ZrO₂ metal oxide catalyst was synthesized *via* the combustion method and was further functionalized with sulphate (SO₄²⁻) groups. The morphology, surface functionalities, and composition of the metal oxide catalyst were determined by scanning electron microscopy, N₂ adsorption and desorption measurement, X-ray diffraction, and Fourier transform infrared spectroscopy. The synthesized catalyst was used for esterification of glycerol with acetic acid. Effects of the process parameters including acetic acid to glycerol molar ratios (3-20), catalyst loadings (1-9 wt.%) and reaction temperatures (70–110°C) on the glycerol conversion and glycerol acetates selectivity were studied. Excellent catalytic activity was observed by using the sulphated metal oxide catalyst resulting in a glycerol conversion as high as 99.12%. The selectivity towards the di and triacetin (fuel additive) formed stood at 57.28% and 21.26% respectively. The reaction rate constants and activation energies were also estimated using a Quasi-Newton algorithm, namely Broyden's method and Arrhenius equations at 80-110°C. The calculated values were in accordance with the experimental values which confirmed the model. Finally, the developed catalyst could be reused for three consecutive cycle without major loss of its activity. Overall, the findings presented here could be instrumental to drive future research and commercialization efforts directed toward biodiesel glycerol valorisation into fuel additives.

©2020 BRTeam CC BY 4.0

* Corresponding author at: Tel.: +91-80-23600822
 E-mail address: rmkulkarni@msrit.edu

Nomenclatures

$k_1, k_2, \text{ and } k_3$	Apparent kinetic rate constants
$-r_G$	Rate of consumption of glycerol ($\text{mol}\cdot\text{min}^{-1}\cdot\text{L}^{-1}$)
$r_M, r_D, \text{ and } r_T$	Rate of formation ($\text{mol}\cdot\text{min}^{-1}\cdot\text{L}^{-1}$) of the species M, D, and T, respectively
C_G	Concentration of glycerol ($\text{mol}\cdot\text{L}^{-1}$)
$C_M, C_D, \text{ and } C_T$	Concentration ($\text{mol}\cdot\text{L}^{-1}$) of the species M, D, and T, respectively
t	Time (min)
C_G	Concentration of glycerol at $t=0$
T_R	Reaction temperature (K)

Abbreviations

AA	Acetic acid
BET	Brunner-Emmet-Teller
BJH	Barrett, Joyner, and Halenda
D	Diacetin
FID	Flame Ionization Detector
FTIR	Fourier transform infrared spectroscopy analysis
G	Glycerol
GC	Gas Chromatography
M	Monoacetin
PID	Proportional –Integral –Derivative controller
SEM	Scanning Electron Microscope
T	Triacetin
XRD	X-ray Diffraction

1. Introduction

The dearth of fossil fuel reserves, energy security and increasing greenhouse gas emissions have fuelled the search for green and clean energy alternatives (Reddy et al., 2010). Biodiesel has gained prominence owing to its various advantages over fossil-oriented counterpart, including biodegradability, non-toxicity, and being environmentally-friendly (Pathak et al., 2010; Aghbashlo et al., 2018). Vegetable oil, animal fat, microalgal oil, etc., have been utilized to produce biodiesel through the transesterification process (Pradima et al., 2017). More specifically, the transesterification of the afore-mentioned oil feedstocks through catalytic routes produces biodiesel as the main product (90 wt.%) and glycerol as by-product (10 wt.%) (Budzaki et al., 2018). The rapid expansion of the biodiesel industry has, in turn, increased the production of glycerol which is low-cost bio-feed available for value addition (Ishak et al., 2016; Sun et al., 2016). Glycerol (glycerine/1,2,3-propanetriol) contains three hydroxyl groups that can be functionalized through a catalytic process. It can be valorised into value-added products such as chemicals, solvents, polyesters, oxygenated fuel additives, etc. (Mufrodi et al., 2012; Huang et al., 2014; Ghaziaskar et al., 2018; Smirnov et al., 2018; Talebian-Kiakalaieh et al., 2018). Thus, the catalytic conversion of glycerol can contribute to the economic viability of the biodiesel industry.

Glycerol can yield esters of glycerol (mono, di, and triacetins) by the process of acetylation with acetic anhydride, ethyl acetate, acetic acid, etc., in the presence of a suitable catalyst. Acetins have great potentials as fuel additives as they are capable of decreasing particulate matter, carbon monoxide, unregulated aldehyde, and unburned hydrocarbon emissions (Goncalves et al., 2008). Improving cold flow properties and viscosity when introduced into diesel and biodiesel formulations is another advantage of these compounds. They can also be used as an antiknock additive for gasoline. Acetins also find applications as plasticizer, food additive, and solvent in leather tanning

industries, as well as in the manufacture of explosives and biodegradable polyesters (Costa et al., 2013).

Previous studies reported on glycerol esterification accelerated by solid or mineral acid catalysts under high temperature and pressure conditions leading to the formation of acetins in moderate to good yields with long reaction times (Khayoon et al., 2011). Mineral acid catalysts such as hydrofluoric acid, sulphuric acid, hydrochloric acid, or acidic ionic liquids were explored for obtaining acetins (Malaika et al., 2019). However, due to limitations like excessive catalyst usage, non-recyclability, serious environmental impacts and corrosion of the equipment, these liquid acids were replaced by solid catalysts. The most widely used catalysts include amberlyst 15, 35 or 36, acid exchange resins, hetero-polyacids, HZSM-5 zeolite, niobium –zirconium mixed oxides, mesoporous silica, HUSY zeolite, and enzymes (Melero et al., 2007; da Silva et al., 2009; Liao et al., 2009; Janaun et al., 2010; Popova et al., 2014; Oh et al., 2015; Rastegari et al., 2015; Betiha et al., 2016; Liu et al., 2019; Pradima et al., 2019). Investigations suggest that hetero-polyacids and amberlyst exhibited poor regeneration ability, thermal stability, etc. While metal oxide catalysts provide various advantages over the above-mentioned catalysts, i.e., being inexpensive, stable, regenerable, and active over a wide range of temperatures (Sudarsanam et al., 2019). Among these metal oxides catalysts, CeO_2 and ZrO_2 are widely considered favourable for their redox properties and ability to form non-stoichiometric mixed metal oxides. They, not only exhibit increased thermal stability but can withstand high pressures with reduced acid site deactivation (Ibrahim et al., 2019; Shah et al., 2019). Furthermore, the substitution of sulphate groups can increase the acid sites for enhanced performance of the catalyst. Functionalized zirconia metal oxide catalyst ($\text{H}_2\text{SO}_4/\text{ZrO}_2$) for glycerol esterification was reported for high selectivity and conversion (Wang et al., 2012).

It is worth noting that although cerium-zirconium oxides have widely been applied in exhaust gas purification, they have rarely used in the synthesis of fine chemicals. To the best of our knowledge, cerium-zirconium oxide catalyst prepared by combustion method has not been tested for the synthesis of biofuel additives. Therefore, in this study, sulphated cerium-zirconium metal oxide catalyst was prepared by the combustion method and was used for glycerol acetylation reaction. The effects of different parameters such as glycerol to acetic acid molar ratio, catalyst loading, and reaction temperature on the product distribution (acetins) were investigated. The prepared catalyst was characterised by means of X-ray diffraction (XRD), scanning electron microscope (SEM), Brunner-Emmet-Teller (BET) surface area, and Fourier transform infrared (FTIR) spectroscopy analysis. In addition, kinetic modelling and analysis were performed to fit the experimental data obtained at different temperatures. A possible reaction mechanism has also been proposed to explain the process, based on the findings of the present study.

2. Materials and Methods**2.1. Materials and reagents**

Glycerol, cerous nitrate ($\text{CeN}_3\text{O}_9\cdot 6\text{H}_2\text{O}$), zirconium nitrate ($\text{Zr}(\text{NO}_3)_4\cdot 5\text{H}_2\text{O}$), urea ($\text{CO}(\text{NH}_2)_2$), sulphuric acid, and acetic acid used were of analytical grade procured from commercial sources. Monoacetin, diacetin, and triacetin pure samples used as standard samples were purchased from Sigma Aldrich (Germany).

2.2. Synthesis of CeO_2 - ZrO_2 mixed oxide catalyst

CeO_2 - ZrO_2 mixed oxide catalyst was synthesized by the combustion method using urea as a reductant and metal nitrates as oxidizers. Predetermined stoichiometry quantities of cerium nitrate ($\text{CeN}_3\text{O}_9\cdot 6\text{H}_2\text{O}$), zirconium nitrate ($\text{Zr}(\text{NO}_3)_4\cdot 5\text{H}_2\text{O}$), and solid Urea ($\text{CO}(\text{NH}_2)_2$) were dissolved in distilled water thoroughly to obtain an aqueous solution. This mixture was heated in a muffle furnace to 500°C . Within 20 min of combustion, a foamy yellow powder was obtained. The synthesized powder was then calcined in the muffle furnace at 300°C for 2 h to produce CeO_2 - ZrO_2 mixed oxide catalyst.

The obtained mixed oxide CeO_2 - ZrO_2 catalyst was used for the acetylation reaction. A portion of the catalyst was sulphated to increase the acid sites. Sulphuric acid (0.5 M) was added to the mixture and stirred over

a magnetic stirrer at 100°C, 500 rpm for an hour, dried in a hot air oven and finally calcined at 300°C for 2 h.

2.3. Catalyst characterization

Powder XRD characterization of the catalyst was recorded on a Bruker JDX 8030 phaser X-ray diffractometer using Copper K α radiation ($\lambda=0.15406$ nm) with a high-resolution Lynxeye detector. The intensity data was collected over a 2θ range of 2–80° with a step size of 0.02°. The counting time was 1°/min. The FTIR spectroscopy analysis was recorded on a Bruker Alpha spectrometer over the range of 400 – 4000 cm^{-1} . Scanning electron microscope (SEM) images for the prepared catalysts were recorded on an ESEM Quanta 200 instrument with a tungsten-based filament for the elemental analysis to investigate the morphology. BET surface areas, pore volume, and average pore diameter of the catalyst were obtained through the N₂ (77K) adsorption measurement using a BELSORP system. The samples were pre-treated at 300°C under vacuum for 2 h before measurement. The average pore diameters were calculated according to the Barrett, Joyner, and Halenda (BJH) model in absorption and desorption.

2.4. Acetylation of glycerol using metallic oxide as catalyst

The acetylation reactions of glycerol with acetic acid was performed in a 100 mL three-necked round bottom flask. This flask was equipped with a magnetic stirrer, a Liebig condenser, a thermometer, and a Proportional-Integral-Derivative (PID) controller. Water was constantly circulated to avoid evaporation of reactants under atmospheric pressure. The glass reactor was placed in an oil bath to ensure uniform heating. The reaction was performed under constant stirring. At regular intervals, a known quantity of the reaction mixture was drawn out and centrifuged for 10 min to separate out the solid catalyst. The supernatant collected was analysed using gas chromatography (GC).

Quantitative analysis of the products was performed on a GC with a flame ionization detector (FID). A silphenylene polysiloxane capillary column (30 m, 250 μm , 0.25 μm) was used. Both the injector and detector were held at a constant temperature of 250°C. Initially, 0.5 μL of the sample was injected at 120°C oven temperature and then was raised up to 150°C, with the rate of 6°C min^{-1} and held for 1 min. Nitrogen was used as a carrier gas at 35 $\text{mL}\cdot\text{min}^{-1}$. The products mono, di, and triacetins were identified based on their retention times using the GC which was pre-calibrated. Calibration was done using pure samples of mono, di, and triacetin. The products formed were determined by relative peak areas.

3. Results and Discussion

3.1. Performance of unsulphated and sulphated cerium/zirconium metal oxide for acetylation of glycerol

The catalytic performance of unsulphated and sulphated cerium/zirconium metal oxide solid catalysts for acetylation of glycerol with acetic acid was investigated. The reaction conditions were maintained as glycerol/acetic acid molar ratio of 1:10, catalyst loading of 5 wt.%, and at 100°C temperature. The obtained experimental results for a reaction time of 3 h are summarized in Table 1. For the same reaction conditions, a blank experiment was performed for esterification reaction of glycerol with acetic acid and a conversion rate of 22% with only one product, i.e., monoacetin was detected (Table 1). Similar observations on reduced glycerol conversion under homogeneous catalysis conditions were reported by Goncalves et al. (2012) and Betiha et al. (2016). Using heterogeneous catalysts several drawbacks associated with application of homogeneous catalysts, i.e., corrosion of the equipment, production of undesired compounds, difficulty in catalyst separation, lack of reusability, environmental hazards, and reduced product purity could be overcome (da Silva et al., 2009; Oh et al., 2015; Betiha et al., 2016; Veluturla et al., 2018). Among the unsulphated and sulphated mixed oxide catalysts, the catalyst containing a higher amount of acid sites ($\text{SO}_4^{2-}/\text{CeO}_2\text{-ZrO}_2$) resulted in the maximum glycerol conversion and was hence selected for further studies.

Figure 1 shows the effect of reaction time variation on the synthesis of acetins using $\text{SO}_4^{2-}/\text{CeO}_2\text{-ZrO}_2$ catalyst. The conversion of glycerol was observed to increase gradually with the increase in reaction time from 0.5 to 5 h. During this period, the selectivity of monoacetin decreased with the increase

Table 1.

Comparison of performance of sulphated and unsulphated $\text{CeO}_2\text{-ZrO}_2$ catalyst for acetylation of glycerol and acetic acid.

Sl. No	Catalyst	Conversion (%)	Selectivity (%)		
			Monoacetin	Diacetin	Triacetin
1	$\text{CeO}_2\text{-ZrO}_2$	57.96	85.39	14.13	0.48
2	$\text{SO}_4^{2-}/\text{CeO}_2\text{-ZrO}_2$	99.12	21.46	57.28	21.26
3	Blank	22.00	100	-	-

in time while the selectivity of diacetin and triacetin increased with increase in time. This confirms that the glycerol acetylation reaction is a series reaction (Zhou et al., 2013; Gao et al., 2015). Glycerol conversion and product selectivity remained almost unchanged after 3 h. Hence, the influence of other parameters was studied throughout a 3-h duration.

The synthesis of acetins by the acetylation reaction proceeds by the activation of the carbonyl group of acetic acid through the transfer of a proton from the metal oxide catalyst resulting in an increased positive charge. The protonated acetic acid is then attacked by the oxygen of glycerol, forming monoacetin with the loss of one water molecule. The monoacetin formed gives diacetin and triacetin in a series reaction (Sandesh et al., 2015).

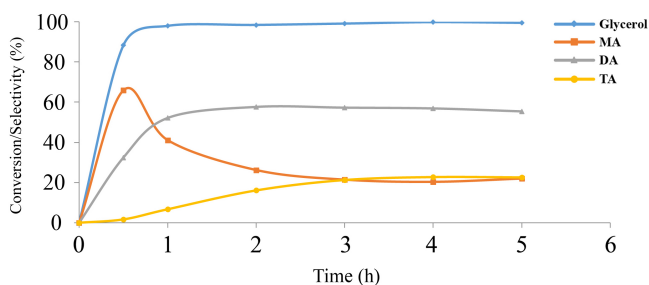


Fig. 1. Effect of time during the acetylation of glycerol with $\text{SO}_4^{2-}/\text{CeO}_2\text{-ZrO}_2$ catalyst at glycerol/acetic acid molar ratio of 1:10, catalyst loading of 5 wt.% at 100 °C.

3.2. Influence of reaction conditions on esterification reaction of glycerol with acetic acid

When glycerol is esterified with acetic acid, some or all of the hydroxyl groups in the glycerol molecules react. Thus, depending on the extent of the reaction, ester isomers are formed: monoacetin, diacetin, and triacetin. The influence of various reaction parameters such as reactants molar ratio, catalyst loading, and reaction temperature using $\text{SO}_4^{2-}/\text{CeO}_2\text{-ZrO}_2$ catalyst during the esterification of glycerol with acetic acid was studied.

3.2.1. Effect of reactants molar ratio

Reaction rates can be increased by introducing one of the reactants in excess (Mufrodi et al., 2014). Effect of five different molar ratios of glycerol to acetic acid, i.e., 1:3, 1:6, 1:10, 1:15, and 1:20 was studied for the conversion of glycerol to mono, di, and triacetin. The reaction conditions were the temperature of 100°C, catalyst loading of 5 wt.%, reaction volume of 25 mL, and reaction time of 3 h (Fig. 2). The conversion of glycerol was increased with varying glycerol/acetic acid molar ratio up to the ratio of 1:10, where the conversion obtained was 99.12% at 3 h. Since acetylation of glycerol is a reversible reaction, the excess availability of acetic acid in the reaction mixture drives the reaction towards the formation of di and triacetins (Tao et al., 2015). The graph clearly indicates the positive effect of an increase in glycerol/acetic acid molar ratio in the reaction mixture on the selectivity towards the formation of diacetin and triacetin. The selectivity of diacetin was enhanced from 42.62% at 1:3 molar ratio to 57.28% at 1:10 molar ratio. The optimum conversion of 99.12

% was achieved at the glycerol/acetic acid ratio of 1:10. Since an equilibrium conversion was achieved at 1:10, no further changes in glycerol conversion were observed at higher molar ratios investigated, i.e., 1:15 and 1:20. Another reason could be that, with an increased molar ratio, more acetic acid molecules would attach to the same active sites of the catalyst (Yadav et al., 2004). These data patterns correlated with those already reported in the literature as well (Balaraju et al., 2010; Pathak et al., 2010; Khayoon et al., 2011; Wang et al., 2016).

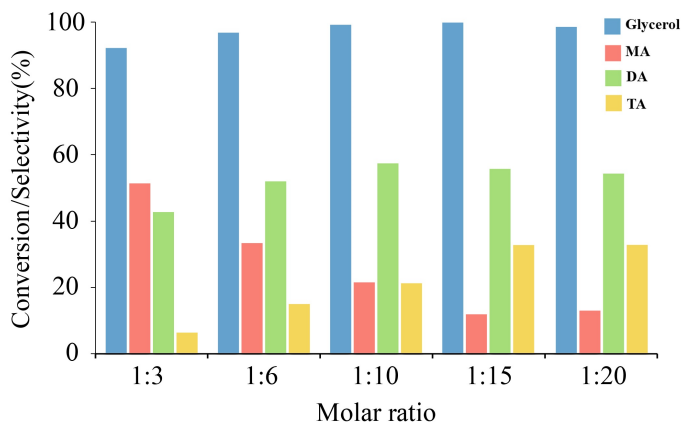


Fig. 2. Effect of glycerol/acetic acid molar ratio on the acetylation of glycerol with acetic acid by using $\text{SO}_4^{2-}/\text{CeO}_2\text{-ZrO}_2$.

3.2.2. Effect of catalyst loading

The effect of catalyst loading was studied at the glycerol/acetic acid molar ratio of 1:10 at 100°C for 3 h. The catalyst loading was varied from 1 to 9 wt.% (Fig. 3). The glycerol conversion was found to increase (95.88% to 99.11%) with increasing catalyst concentration from 1 to 5 wt.%. For the catalyst loading of 1 wt.%, selectivity towards mono, di, and triacetin was 39.14%, 53.54%, and 7.32%, respectively. Whereas, for 5 wt.% catalyst, selectivity towards the three acetins was 21.46%, 57.28%, and 21.26% respectively. However, a further increase in catalyst loading led to no significant variation in glycerol conversion and yield of acetins. A similar trend was also observed by Sandesh et al. (2015) and Okoye et al. (2017).

The formation of acetins was increased with increasing catalyst loading due to the availability of more active sites. Initially, an increase in catalyst concentration accelerated the rate of reaction and enhanced product formation but with further increases in catalyst concentration, the particles tended to agglomerate reducing the accessibility of the reactants to the catalyst. The active sites situated on the surface of such agglomerates actively participate in forming products hindering transfer rates to active sites inside the aggregates (Setyaningsih et al., 2018).

3.2.3. Effect of reaction temperature

The effect of reaction temperature (70°C to 110°C) on glycerol conversion and product selectivity (Fig. 4) was studied at the glycerol/acetic acid molar ratio of 1:10 and 5 wt.% catalyst loading for 3 h reaction time. In general, increasing temperature may result in increased interaction between reactants and catalyst, reduce viscosity, and enhance solubility. It could also improve the diffusion of reactants and products in and out of the active sites. Acetylation reactions are endothermic. Selectivity is temperature-dependent and that explains the formation of mainly monoacetin at low temperatures. By increasing the temperature, at the expense of monoacetin and diacetin, the selectivity of triacetin increased drastically. This indicates the dependence on temperature favoring conversion of monoacetin and diacetin to triacetin (Tao et al., 2015). Catalytic activity was found to be best at 100°C for the glycerol and acetic acid esterification reaction. At 110°C, glycerol conversion remained the same but with increased selectivity towards triacetin formation (24.59%). A similar trend was reported by Wang et al. (2016). A higher temperature is known to aid triacetin formation and alter/shift the equilibrium towards the

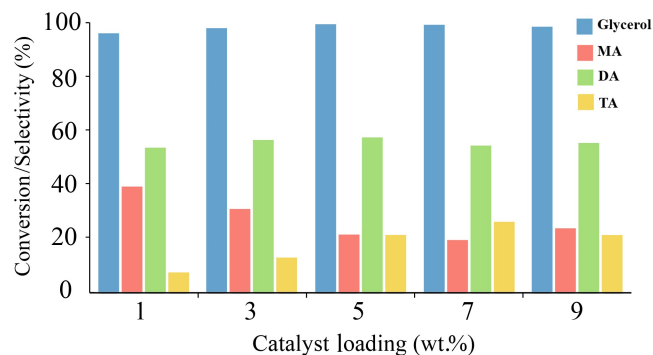


Fig. 3. Effects of varying catalyst loadings on glycerol conversion and product selectivity during the acetylation of glycerol with acetic acid by using $\text{SO}_4^{2-}/\text{CeO}_2\text{-ZrO}_2$.

formation of reactants at the same time (Liao et al., 2009; Gao et al., 2015). With further increase in temperature above 110°C, selectivity towards the formation of acetins was found to decrease. This can be attributed to the reduced availability of acetic acid which tends to evaporate at a higher rate (Mufrodi et al., 2014). A comparison of the efficiency of $\text{SO}_4^{2-}/\text{CeO}_2\text{-ZrO}_2$ in glycerol conversion and acetin selectivity with different catalysts used in various research works is presented in Table 2.

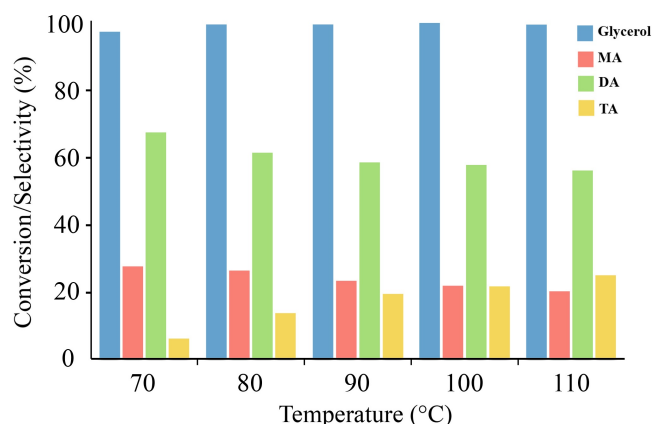


Fig. 4. Effects of varying temperature on glycerol conversion and product selectivity during the acetylation of glycerol with acetic acid by using $\text{SO}_4^{2-}/\text{CeO}_2\text{-ZrO}_2$.

3.3. Catalyst characterization

3.3.1. XRD analysis of mixed metal oxide catalyst

The XRD pattern of sulphated cerium and zirconium metal oxide catalyst showed a diffraction peak corresponding to cubic, fluorite-type crystalline structure (Fig. 5). The characteristic peaks, cubic crystalline phase with reflections at $2\theta = 28.8, 33.1, 47.6,$ and 56.6 exhibited by $\text{SO}_4^{2-}/\text{CeO}_2\text{-ZrO}_2$ indicated a true metal oxide phase. Characteristic peaks corresponding to the CeOSO_4 phase were also exhibited by the catalyst. Furthermore, the formation of different types of surface zirconium sulphates [$\text{Zr}(\text{SO}_4)_2$, $\text{Zr}(\text{SO}_4)_2 \cdot 4\text{H}_2\text{O}$, and $\text{Zr}(\text{SO}_4)_2 \cdot 5\text{H}_2\text{O}$] were observed. Similar observations were made for the $\text{SO}_4^{2-}/\text{CeO}_2\text{-ZrO}_2$ catalyst prepared by the precipitation method (Reddy et al., 2012).

3.3.2. FT-IR analysis

Figures 6a and 6b show the IR spectra of the catalytic materials $\text{SO}_4^{2-}/\text{CeO}_2\text{-ZrO}_2$ and $\text{CeO}_2\text{-ZrO}_2$ catalyst. The characteristics peaks of the

Table 2. Comparison of the efficiency of the mixed metal oxide catalyst ($\text{SO}_4^{2-}/\text{CeO}_2\text{-ZrO}_2$) developed in the present study with different catalysts reported previously in terms of glycerol conversion and selectivity.

Reactants	Catalysts	Reaction parameters				X_G^* (%)	Selectivity (%)			Reference
		MR	Catalyst loading	Time (h)	Temp. (°C)		MA	DA	TA	
Glycerol and acetic anhydride	Magnetic solid acid catalysts (Fe-Sn-Ti(SO_4^{2-})-400)	Gly -1.5g, acetic anhydride -8.39 g	0.05 g	0.5	80	99	13	61	26	Sun et al. (2016)
Glycerol and acetic acid	Amberlyst 35	1:9	0.5 g	4	105	100	50	15	35	Liao et al. (2009)
Glycerol and acetic acid	Solid acid catalyst (SBA-15)	1:9	0.7 g	6	110	95	19	59	22	Goscianska et al. (2019)
Glycerol and acetic acid	Amberlyst 15	1:9	5 Wt.%	5	110	97	7	48	45	Zhou et al. (2012)
Glycerol and acetic acid	Al-clays	1:3	1 g	1	120	60	41	10	9	Venkatesha et al. (2016)
Glycerol and acetic acid	Propyl- SO_3H functionalized SBA-15 (SSBA)	1:3	0.05 g	3	105	100	5	62	33	Testa et al. (2013)
Glycerol and acetic acid	Metal oxides	1:6	0.5 g of 7% alumina loaded graphene oxide	2	120	97	26	27	47	Kanimozhi et al. (2018)
Glycerol and acetic acid	Solid acid catalysts (SAR)	1:3	75 mg	6	80	10	22	66	12	Neto et al. (2018)
Glycerol and acetic acid	Solid acid catalysts (SAC)	1:3	75 mg	6	80	7	19	63	18	Neto et al. (2018)
Glycerol and acetic acid	Mixed metal oxides ($\text{SO}_4^{2-}/\text{CeO}_2\text{-ZrO}_2$)	1:10	5 wt.%	3	100	99	22	57	21	This work

* X_G : Glycerol conversion

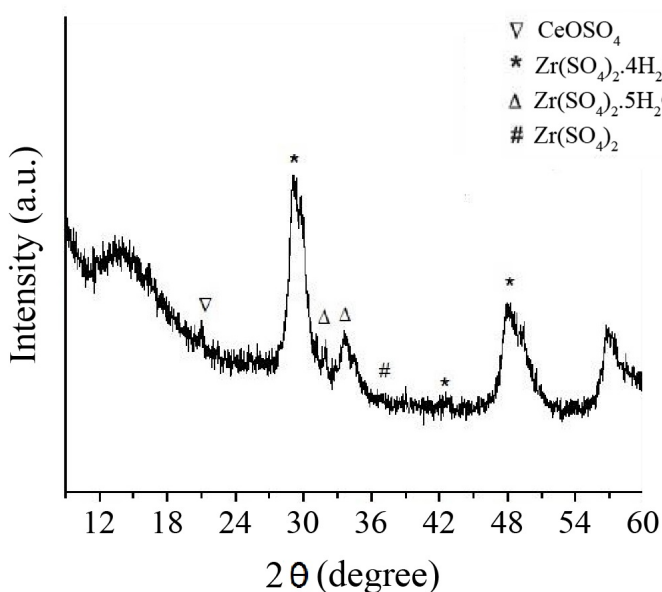


Fig. 5. X-ray diffraction pattern of the $\text{SO}_4^{2-}/\text{CeO}_2\text{-ZrO}_2$ catalyst.

sulphated metal oxides often occur between 900 to 1400 cm^{-1} and are assigned to the stretching vibrations of the S=O or S-O bond (Sandesh et al., 2015; Sun et al., 2016).

3.3.3. BET analysis

Morphological properties of the metal oxide catalyst derived from nitrogen physisorption isotherms showed the Brunauer's type IV isotherm (Fig. 7a) indicating a characteristic range of high mesoscopic ordering of molecules with the surface area of $22.07\text{ m}^2/\text{g}$ (Fig. 7b) and a mean pore diameter of 5.90 nm . The isotherm indicated that maximum attachment occurred before the saturation pressure was reached.

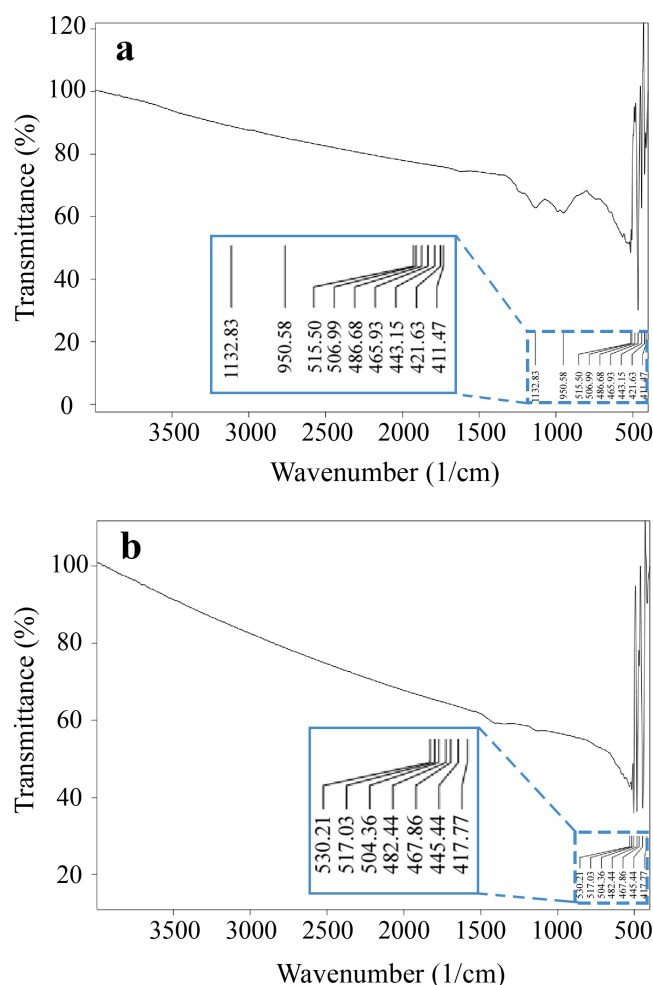


Fig. 6. FT-IR spectra of the (a) $\text{SO}_4^{2-}/\text{CeO}_2\text{-ZrO}_2$ and (b) $\text{CeO}_2\text{-ZrO}_2$ catalyst.

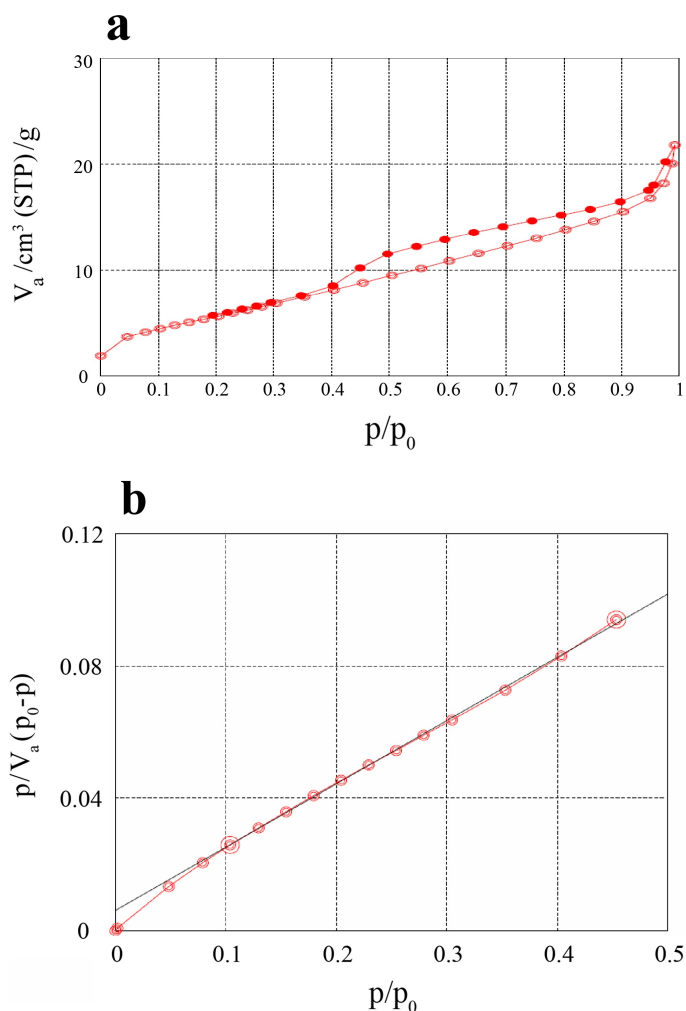


Fig. 7. (a) The plot of N₂ adsorption-desorption isotherm for the SO₄²⁻/CeO₂-ZrO₂ catalyst recorded at 77 K and (b) BET isotherm plot for the SO₄²⁻/CeO₂-ZrO₂ catalyst.

3.3.4. SEM analysis of the catalyst

The morphology of SO₄²⁻/CeO₂-ZrO₂ and CeO₂-ZrO₂ mixed oxide catalysts were investigated by the SEM. The sulphated sample appeared as irregular particles formed from aggregates of randomly oriented smaller particles but with no defined crystal shapes as seen in Figure 8a. On the other hand, the unsulphated sample was composed of clear pellet-like particles and the particles were uniformly scattered as shown in Figure 8b.

3.4. Kinetic Analysis

A suitable model was developed to fit the kinetic rate data obtained from the effect of temperature studies (80-110°C) for the solid catalyzed acetylation reaction. A kinetic scheme suggested by Gelosa et al. (2003) was used to describe the series reaction (Eq. 1).



Zhou et al. (2012) proposed a simplified scheme by considering a pseudo homogenous model devoid of limitations posed by mass transfer and equilibrium. This is ascribed to the weak adsorption on the catalyst and a slow backward reaction. In addition, glycerol was assumed to be the limiting reagent due to high molar ratios of acetic acid [AA] to glycerol [G]. This proves to be a valid assumption as the excess acetic acid is required to convert monoacetin [M] to diacetin [D] and further from diacetin to triacetin [T]. The differential rate of reaction as proposed by Zhou et al. (2012) for the four components involved are as follows (Eqs. 2-5):

$$-r_G = -\frac{dC_G}{dt} = k_1 C_G \quad (\text{Eq. 2})$$

$$r_M = \frac{dC_M}{dt} = k_1 C_G - k_2 C_M \quad (\text{Eq. 3})$$

$$r_D = \frac{dC_D}{dt} = k_2 C_M - k_3 C_D \quad (\text{Eq. 4})$$

$$r_T = \frac{dC_T}{dt} = k_3 C_D \quad (\text{Eq. 5})$$

Since there is no product formed in the reactor at the start of the reaction, the initial concentration of species M, D, and T are zero.

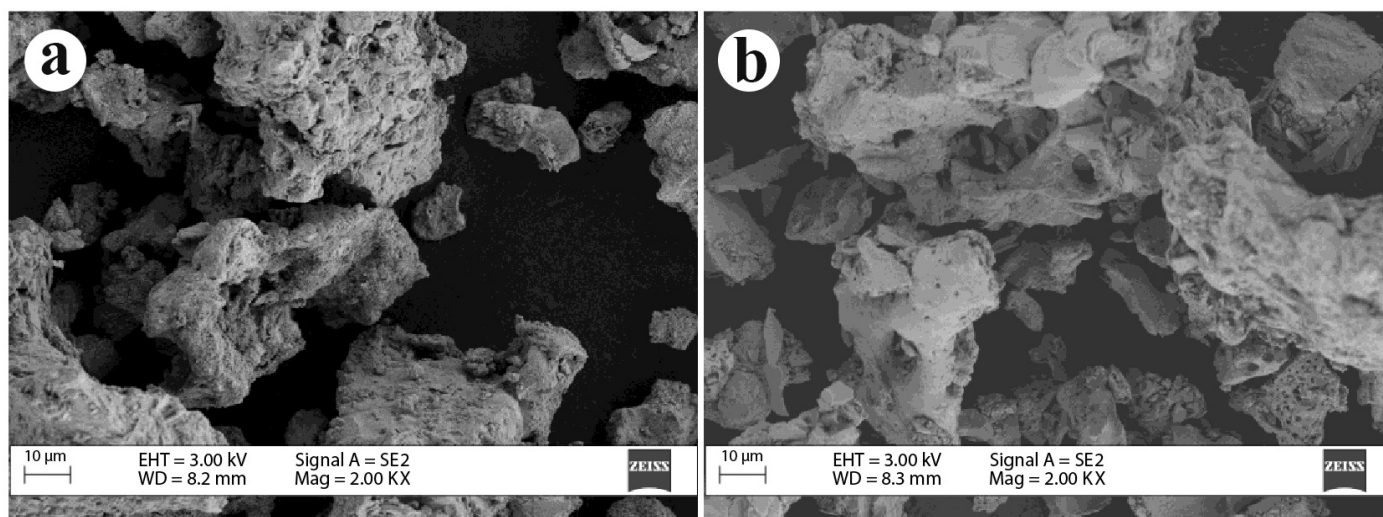


Fig. 8. (a) The SEM image of the (a) SO₄²⁻/CeO₂-ZrO₂ and (b) CeO₂-ZrO₂ catalyst.

By integrating Equations 2-5, the following yield expressions were obtained (Eqs. 6-9):

$$\frac{C_G}{C_G} = e^{-k_1 t} \quad (\text{Eq. 6})$$

$$\frac{C_M}{C_G} = \frac{k_1}{k_2 - k_1} (e^{-k_1 t} - e^{-k_2 t}) \quad (\text{Eq. 7})$$

$$\frac{C_D}{C_G} = \frac{k_1 k_2}{k_2 - k_1} \left(\frac{e^{-k_1 t}}{k_3 - k_1} - \frac{e^{-k_2 t}}{k_3 - k_2} + \frac{(k_2 - k_1)e^{-k_3 t}}{(k_3 - k_2)(k_3 - k_1)} \right) \quad (\text{Eq. 8})$$

$$\frac{C_T}{C_G} = k_1 k_2 k_3 \left(\frac{1 - e^{-k_1 t}}{k_1(k_1 - k_2)(k_1 - k_3)} + \frac{1 - e^{-k_2 t}}{k_2(k_2 - k_1)(k_2 - k_3)} + \frac{1 - e^{-k_3 t}}{k_3(k_3 - k_1)(k_3 - k_2)} \right) \quad (\text{Eq. 9})$$

In order to obtain the kinetic rate constants and activation energies of the series reaction system, a Quasi-Newton algorithm, namely Broyden's method was employed. The solutions were the optimized values which minimized the root mean square difference between the experimental and predicted yields by Equations 6-9. The results obtained are displayed in Table 3.

Table 3.
Values of apparent rate constants at different reaction temperatures.

Temperature (°C)	k ₁ (min ⁻¹)	k ₂ (min ⁻¹)	k ₃ (min ⁻¹)
80	0.0718	0.0126	0.0046
90	0.0782	0.0147	0.0066
100	0.0791	0.0170	0.0102
110	0.0813	0.0195	0.0150

Temperature plays a major role in heterogeneous catalysis and the temperature dependence of the rate constants can be given by the Arrhenius equation. A plot of log (k_i) vs. 1/T_R (Fig. 9) displays a linear behaviour and the activation energy values of 5.34, 16.40, and 43.57 kJ.mol⁻¹ were calculated for the formation of monoacetin, diacetin, and triacetin, respectively.

Pankajakshan et al. (2018) reported the kinetic parameters for glycerol acetylation using a sulphated γ-Al₂O₃ catalyst. The very high activation energy for the third reaction and low value of rate constant could explain the lower yield of triacetin obtained by the authors. In contrast, the lower values of activation energy and higher values of rate constant for the first and second reaction favoured the faster formation of monoacetin and diacetin. The high yield of diacetin can also be attributed to the direct acetylation of glycerol in the early phases as suggested by the reaction mechanisms proposed in the literature (Pankajakshan et al., 2018).

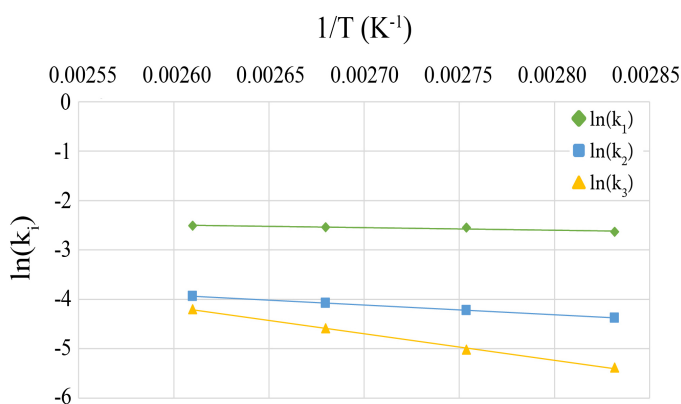


Fig. 9. Arrhenius plot in the temperature range of 80-110°C.

3.5. Catalyst reusability studies

The reusability of the metal oxide catalyst was also examined. For each cycle, the optimum conditions for maximum conversion of glycerol were determined and discussed above. The catalyst showed a good recyclability with a similar activity for three cycles. After the reaction, the solid catalyst was separated from the reaction mixture, washed with ethyl acetate to remove residual glycerol and other products. The catalyst was then dried in a hot air oven at 100°C followed by activation at 150°C in the muffle furnace. The obtained metal oxide catalyst was used for the next run by adding reactants. Glycerol conversion decreased by 5% with each run. The selectivity towards the acetins formation was almost the same for the three cycles. However, both the conversion rate and selectivity decreased drastically at the fourth cycle. More specifically, glycerol conversion stood at 76.7% while the selectivity towards mono, di, and triacetin were recorded at 76%, 22.6%, and 1.4% respectively. Therefore, based on the results obtained the metal oxide catalyst investigated was found efficient and could be recycled up to three cycles.

4. Conclusions and future directions

The glycerol acetylation reaction with acetic acid was carried out over unsulphated and sulphated CeO₂-ZrO₂ mixed oxide catalysts. The effects of various parameters such as reaction time, glycerol/acetic acid molar ratio, catalyst loading, and temperature on glycerol conversion and selectivity towards product formation were scrutinized. It was observed that sulphated CeO₂-ZrO₂ mixed oxide catalyst exhibited a favourable performance in comparison with the unsulphated catalyst. The highest glycerol conversion of 99.12 % with high selectivity towards di and triacetins (57.28 % and 21.26%, respectively) was achieved at 100°C and for 3 h of reaction time. The inexpensive CeO₂-ZrO₂ metal oxide catalyst prepared by the combustion method was found stable, reusable, and sustainable over a wide range of temperatures. A kinetic model was developed based on the experimental data at 80-110°C by using the Broyden's method and Arrhenius equations. The activation energy of 5.34, 16.40, and 43.57 kJ.mol⁻¹ was obtained for monoacetin, diacetin, and triacetin respectively. It was observed that the high activation energy for the formation of triacetin led to lower yield while the comparatively lower activation energies resulted in the formation of mono and diacetin with greater yields. Future work should focus on consolidating these results to be applicable for scale-up studies on glycerol acetylation reaction. Different flow reactor configurations, modification of catalyst surface and their application towards glycerol transformation should also be explored. Finally, the results obtained can be integrated into a single framework and recommended for a better understanding of scale-up reactors.

Acknowledgements

We gratefully acknowledge, 1) The Institution of Engineers (India) (DR2017003), 2) Karnataka State Council for Science and Technology, and 3) Vision Group on Science and Technology (VGST/GRD-691) for the financial support. We would also like to extend our appreciations to the Department of Chemical Engineering, MSRIT, Bangalore.

References

- [1] Aghbashlo, M., Tabatabaei, M., Rastegari, H., Ghaziaskar, H.S., 2018. Exergy-based sustainability analysis of acetins synthesis through continuous esterification of glycerol in acetic acid using Amberlyst® 36 as catalyst. *J. Cleaner Prod.* 183, 1265-1275.
- [2] Balaraju, M., Nikhitha, P., Jagadeeswaraiyah, K., Srilatha, K., Prasad, P.S., Lingaiah, N., 2010. Acetylation of glycerol to synthesize bioadditives over niobic acid supported tungstophosphoric acid catalysts. *Fuel Process Technol.* 91(2), 249-253.
- [3] Betiha, M.A., Hassan, H.M., El-Sharkawy, E.A., Al-Sabagh, A.M., Menoufy, M.F., Abdelmoniem, H.M., 2016. A new approach to polymer-supported phosphotungstic acid: application for glycerol acetylation using robust sustainable acidic heterogeneous-homogenous catalyst. *Appl. Catal. B.* 182, 15-25.

- [4] Budżaki, S., Miljić, G., Sundaram, S., Tišma, M., Hessel, V., 2018. Cost analysis of enzymatic biodiesel production in small-scaled packed-bed reactors. *Appl. Energy*. 210, 268-278.
- [5] Costa, I.C., Itabaiana Jr, I., Flores, M.C., Lourenço, A.C., Leite, S.G., de M. e Miranda, L.S., Leal, I.C., de Souza, R.O., 2013. Biocatalyzed acetins production under continuous-flow conditions: valorization of glycerol derived from biodiesel industry. *J. Flow. Chem.* 3(2), 41-45.
- [6] da Silva, C.X., Gonçalves, V.L., Mota, C.J., 2009. Water-tolerant zeolite catalyst for the acetalisation of glycerol. *Green Chem.* 11(1), 38-41.
- [7] Gao, X., Zhu, S., Li, Y., 2015. Graphene oxide as a facile solid acid catalyst for the production of bioadditives from glycerol esterification. *Catal. Commun.* 62, 48-51.
- [8] Gelosa, D., Ramaioli, M., Valente, G., Morbidelli, M., 2003. Chromatographic reactors: esterification of glycerol with acetic acid using acidic polymeric resins. *Ind. Eng. Chem. Res.* 42(25), 6536-6544.
- [9] Ghaziaskar, H.S., Gorji, Y.M., 2018. Synthesis of solketalacetin as a green fuel additive via ketalization of monoacetin with acetone using silica benzyl sulfonic acid as catalyst. *Biofuel Res. J.* 5(1), 753-758.
- [10] Gonçalves, V.L., Pinto, B.P., Silva, J.C., Mota, C.J., 2008. Acetylation of glycerol catalyzed by different solid acids. *Catal. Today*. 133, 673-677.
- [11] Gonçalves, C.E., Laier, L.O., Cardoso, A.L., da Silva, M.J., 2012. Bioadditive synthesis from $H_3PW_{12}O_{40}$ -catalyzed glycerol esterification with HOAc under mild reaction conditions. *Fuel Process Technol.* 102, 46-52.
- [12] Goscianska, J., Malaika, A., 2019. A facile post-synthetic modification of ordered mesoporous carbon to get efficient catalysts for the formation of acetins. *Catal. Today*.
- [13] Huang, M.Y., Han, X.X., Hung, C.T., Lin, J.C., Wu, P.H., Wu, J.C., Liu, S.B., 2014. Heteropolyacid-based ionic liquids as efficient homogeneous catalysts for acetylation of glycerol. *J. Catal.* 320, 42-51.
- [14] Ifrah, S., Li, W., Buissette, V., Denaire, S., Coelho, J., Miguel, M.R., 2019. Cerium-and zirconium-based mixed oxides. U.S. Patent Application 16/096,279.
- [15] Ishak, Z.I., Sairi, N.A., Alias, Y., Aroua, M.K.T., Yusoff, R., 2016. Production of glycerol carbonate from glycerol with aid of ionic liquid as catalyst. *Chem. Eng. J.* 297, 128-132.
- [16] Janaun, J., Ellis, N., 2010. Glycerol etherification by tert-butanol catalyzed by sulfonated carbon catalyst. *J. Appl. Sci.* 10(21), 2633-2637.
- [17] Kanimozhi, S., Ramani, V., Pandurangan, A., 2018. Effects of alumina on GO and KIT-6 supports for the acetylation of glycerol. *New J. Chem.* 42(23), 18942-18950.
- [18] Khayoon, M.S., Hameed, B.H., 2011. Acetylation of glycerol to biofuel additives over sulfated activated carbon catalyst. *Bioresour. Technol.* 102(19), 9229-9235.
- [19] Liao, X., Zhu, Y., Wang, S.G., Li, Y., 2009. Producing triacetyl glycerol with glycerol by two steps: esterification and acetylation. *Fuel Process Technol.* 90(7-8), 988-993.
- [20] Liu, J., Wang, Z., Sun, Y., Jian, R., Jian, P., Wang, D., 2019. Selective synthesis of triacetin from glycerol catalyzed by HZSM-5/MCM-41 micro/mesoporous molecular sieve. *Chin. J. Chem. Eng.* 27(5), 1073-1078.
- [21] Malaika, A., Kozłowski, M., 2019. Glycerol conversion towards valuable fuel blending compounds with the assistance of SO_3H -functionalized carbon xerogels and spheres. *Fuel Process Technol.* 184, 19-26.
- [22] Melero, J.A., Van Grieken, R., Morales, G., Paniagua, M., 2007. Acidic mesoporous silica for the acetylation of glycerol: synthesis of bioadditives to petrol fuel. *Energy Fuel.* 21(3), 1782-1791.
- [23] Mufrodi, Z., Rochmadi, R., Sutijan, S., Budiman, A., 2014. Synthesis acetylation of glycerol using batch reactor and continuous reactive distillation column. *Eng. J.* 18(2), 29-40.
- [24] Mufrodi, Z., Sutijan, R., Budiman, A., 2012. Chemical kinetics for synthesis of triacetin from biodiesel byproduct. *Int. J. Chem.* 4(2), 101.
- [25] Neto, A.B., Oliveira, A.C., Rodriguez-Castellón, E., Campos, A.F., Freire, P.T., Sousa, F.F., Josué Filho, M., Araujo, J.C., Lang, R., 2018. A comparative study on porous solid acid oxides as catalysts in the esterification of glycerol with acetic acid. *Catal. Today*.
- [26] Oh, S., Park, C., 2015. Enzymatic production of glycerol acetate from glycerol. *Enzyme Microb. Tech.* 69, 19-23.
- [27] Okoye, P.U., Abdullah, A.Z., Hameed, B.H., 2017. A review on recent developments and progress in the kinetics and deactivation of catalytic acetylation of glycerol—A byproduct of biodiesel. *Renew. Sust. Energy Rev.* 74, 387-401.
- [28] Pankajakshan, A., Pudi, S.M., Biswas, P., 2018. Acetylation of glycerol over highly stable and active sulfated alumina catalyst: reaction mechanism, kinetic modeling and estimation of kinetic parameters. *Int. J. Chem. Kinet.* 50(2), 98-111.
- [29] Pathak, K., Reddy, K.M., Bakhshi, N.N., Dalai, A.K., 2010. Catalytic conversion of glycerol to value added liquid products. *Appl. Catal. A.* 372(2), 224-238.
- [30] Popova, M., Szegedi, Á., Ristić, A., Tušar, N.N., 2014. Glycerol acetylation on mesoporous KIL-2 supported sulphated zirconia catalysts. *Catal. Sci. Technol.* 4(11), 3993-4000.
- [31] Pradima, J., Kulkarni, M.R., 2017. Review on enzymatic synthesis of value added products of glycerol, a by-product derived from biodiesel production. *Resource-Efficient Technol.* 3(4), 394-405.
- [32] Pradima, J., Kulkarni, R.M., Narula, A., Sravanthi, V., Rakshith, R., Nizar, N.R., 2019. Synthesis of Acetins from Glycerol using Lipase from wheat extract. *Korean Chem. Eng. Res.* 57(4), 501-506.
- [33] Rastegari, H., Ghaziaskar, H.S., 2015. From glycerol as the by-product of biodiesel production to value-added monoacetin by continuous and selective esterification in acetic acid. *J. Ind. Eng. Chem.* (21), 856-861.
- [34] Reddy, P.S., Sudarsanam, P., Raju, G., Reddy, B.M., 2010. Synthesis of bio-additives: acetylation of glycerol over zirconia-based solid acid catalysts. *Catal. Commun.* 11(15), 1224-1228.
- [35] Reddy, P.S., Sudarsanam, P., Raju, G., Reddy, B.M., 2012. Selective acetylation of glycerol over CeO_2-M and SO_4^{2-}/CeO_2-M ($M=ZrO_2$ and Al_2O_3) catalysts for synthesis of bioadditives. *J. Ind. Eng. Chem.* 18(2), 648-654.
- [36] Sandesh, S., Manjunathan, P., Halgeri, A.B., Shanbhag, G.V., 2015. Glycerol acetins: fuel additive synthesis by acetylation and esterification of glycerol using cesium phosphotungstate catalyst. *RSC Adv.* 5(126), 104354-104362.
- [37] Setyaningsih, L., Siddiq, F., Pramezy, A., 2018. Esterification of glycerol with acetic acid over Lewatit catalyst. In *MATEC Web of Conferences*. 154, 01028.
- [38] Shah, P.M., Day, A.N., Davies, T.E., Morgan, D.J., Taylor, S.H., 2019. Mechanochemical preparation of ceria-zirconia catalysts for the total oxidation of propane and naphthalene Volatile Organic Compounds. *Appl. Catal. B.* 253, 331-340.
- [39] Smirnov, A.A., Selishcheva, S.A., Yakovlev, V.A., 2018. Acetalization catalysts for synthesis of valuable oxygenated fuel additives from glycerol. *Catalysts.* 8(12), 595.
- [40] Sudarsanam, P., Peeters, E., Makshina, E.V., Parvulescu, V.I., Sels, B.F., 2019. Advances in porous and nanoscale catalysts for viable biomass conversion. *Chem. Soc. Rev.* 48(8), 2366-2421.
- [41] Sun, J., Tong, X., Yu, L., Wan, J., 2016. An efficient and sustainable production of triacetin from the acetylation of glycerol using magnetic solid acid catalysts under mild conditions. *Catal. Today.* 264, 115-122.
- [42] Talebian-Kiakalaieh, A., Amin, S., Saidina, N.A., Tarighi, S., Najafii, N., 2018. A review on the catalytic acetalization of bio-renewable glycerol to fuel additives. *Front. Chem.* 6, 573.
- [43] Tao, M.L., Guan, H.Y., Wang, X.H., Liu, Y.C., Louh, R.F., 2015. Fabrication of sulfonated carbon catalyst from biomass waste and its use for glycerol esterification. *Fuel Process Technol.* 138, 355-360.
- [44] Testa, M.L., La Parola, V., Liotta, L.F., Venezia, A.M., 2013. Screening of different solid acid catalysts for glycerol acetylation. *J. Mol. Catal. A.* 367, 69-76.
- [45] Veluturla, S., Narula, A., Rao, D.S., Kulkarni, R.M., 2018. Experimental and Kinetic Studies of Esterification of Glycerol Using Combustion Synthesized $SO_4^{2-}/CeO_2-Al_2O_3$. *Korean Chem. Eng. Res.* 56(4), 592-599.

- [46] Venkatesha, N.J., Bhat, Y.S., Prakash, B.J., 2016. Volume accessibility of acid sites in modified montmorillonite and triacetin selectivity in acetylation of glycerol. *RSC Adv.* 6(51), 45819-45828.
- [47] Wang, L., Liu, Q., Zhou, M., Xiao, G., 2012. Synthesis of glycerin triacetate over molding zirconia-loaded sulfuric acid catalyst. *J. Nat. Gas Chem.* 21(1), 25-28.
- [48] Wang, Z.Q., Zhang, Z., Yu, W.J., Li, L.D., Zhang, M.H., Zhang, Z.B., 2016. A swelling-changeful catalyst for glycerol acetylation with controlled acid concentration. *Fuel Process Technol.* 142, 228-234.
- [49] Yadav, G.D., Murkute., A.D., 2004. Preparation of a novel catalyst UDCaT-5: enhancement in activity of acid-treated zirconia—effect of treatment with chlorosulfonic acid vis-à-vis sulfuric acid. *J. Catal.* 224(1), 218-223.
- [50] Zhou, L., Nguyen, T.H., Adesina, A.A., 2012. The acetylation of glycerol over amberlyst-15: kinetic and product distribution. *Fuel Process Technol.* 104, 310-318.
- [51] Zhou, L., Al-Zaini, E., Adesina, A.A., 2013. Catalytic characteristics and parameters optimization of the glycerol acetylation over solid acid catalysts. *Fuel.* 103, 617-625.